THE JOURNAL OF PHYSICAL CHEMISTRY C

ARTICLE

pubs.acs.org/JPCC

Toward an Understanding of Ligand Selectivity in Nanocluster Synthesis

Sampyo Hong,[†] Ghazal Shafai,[†] Massimo Bertino,[‡] and Talat S. Rahman*[,†]

[†]Department of Physics, University of Central Florida, Orlando, Florida 32816, United States

[‡]Department of Physics, Virginia Commonwealth University, Richmond, Virginia 23284, United States

Supporting Information

ABSTRACT: We performed scalar relativistic density functional theory (DFT) calculations using the projector augmented wave scheme (PAW) to examine the reactivity and selectivity of diphosphine ligands L^M, with the formula $PH_2(CH_2)_MPH_2$ (spacer $M = 3, 5$), toward small-sized cationic Au_n ($n = 7-11$) nanoclusters. By isolating the ligand-induced contribution to the stability condition, we show that such interaction selectively stabilizes the cationic Au_{11} cluster. Furthermore, we find that L^5 with the longer spacer is more capable than L^3 of relieving the strain imposed on the spacer by bidentate binding to gold clusters, which have relatively small Au−Au bond lengths. Thus L^5 can interact effectively with gold clusters of various sizes, but L^3 can do so only with a selected few. This result demonstrates the size-selecting power of L^3 toward small gold clusters such as Au_{11}^{3+}. To further test the validity of our results we have extended the calculation to a larger cluster, Au_{13}, and also considered the case of a ligand with a larger spacer, $M = 10$, interacting with a small cluster (Au_3). We find that, for $Au_{13}(L^3)_6^{5+}$, the strain induced by the stiff L^3 spacer causes the gold cluster to disintegrate. We also predict a single-end binding for the interaction of L^3 with the gold trimer: one end of the diphosphine is detached from the trimer. Finally, for an ideal, highly selective ligand, we propose a two-body ligand system, in which one part of the ideal ligand provides high reactivity toward the broad range of gold clusters and the other part provides control over the reactivity. The controllable competition between the two components of an ideal, highly selective ligand system will produce a desirable selectivity for the generation of monodisperse nanoclusters of interest through tailoring process.

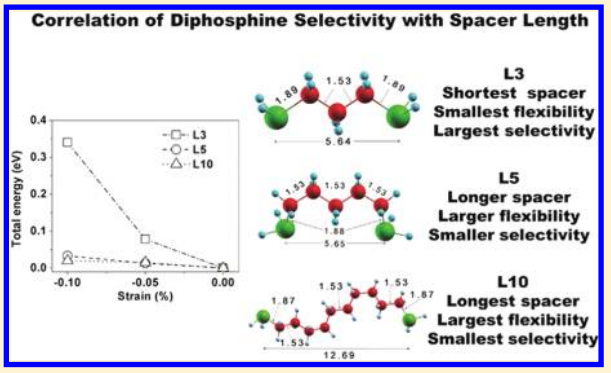

1. INTRODUCTION

Nanoclusters are technologically promising materials. Owing to their large surface-to-volume ratio, nanoclusters exhibit physical and chemical properties that are quite different from those of the bulk counterparts. For example, while bulk gold is inert for chemical reactions, gold nanoclusters show high catalytic reactivity.[1,2] They also exhibit optical characteristics[3] that make them candidates for such potential applications as data storage, ultrafast switching, and gas sensors. Facile synthesis of stable monodisperse gold clusters is therefore of great technological importance. Metal nanoclusters can be synthesized comparatively easily, but their suspensions are generally polydisperse. Monodisperse suspensions are often obtained by filtration procedures that are time-consuming and frequently poor in yield. Furthermore, the synthesis of small-sized monodisperse nanoclusters (typically consisting of fewer than 100 atoms) in large amounts currently presents considerable hurdles. These drawbacks have led to various attempts to develop synthetic procedures that directly produce monodisperse nanocluster suspensions.[4−7] Recently, a simple such method has been developed. This method employs bidentate ligands with the general formula $P(Ph)_2(CH_2)_MP(Ph)_2$, where Ph stands for the phenyl group and M is the length of the aliphatic chain separating the P atoms. Remarkably, the size of the nanoclusters can be controlled by varying M.[8] For example, Au_{11} was generated when a propane spacer was employed, while a mixture of Au_8 and Au_{10} resulted when the spacer was pentane. (We note that Au_8 was also generated by the same ligand with the propane spacer in a similar experiment,[9] indicating that experimental preparation conditions also play a role.) These advances have paved the way for the synthesis of cluster matter in the near future. However, the relationship between the length of the ligand as controlled by the spacer and the size of the cluster that it stabilizes is so far not clear.

In this paper, we use density functional theory (DFT) based calculations to investigate the origin of size selectivity of diphosphine ligands toward small-sized Au clusters. In our previous study of phosphine-protected Au_{13} clusters, we found the strong coupling between the gold and phosphines resulting from charge

Received: February 21, 2011
Revised: June 17, 2011
Published: June 29, 2011

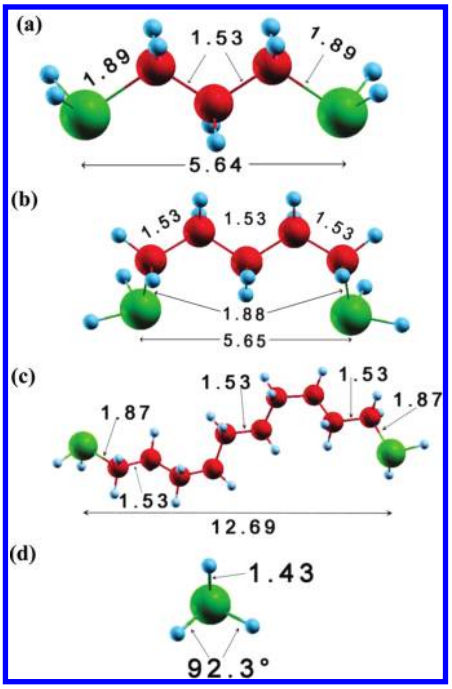

Figure 1. Three types of diphosphine ligands used in this study: (a) $PH_2(CH_2)_3PH_2$ [abbreviated L^3], (b) $PH_2(CH_2)_5PH_2$ [abbreviated L^5], and (c) $PH_2(CH_2)_{10}PH_2$ [abbreviated L^{10}], and (d) phosphine ligand.

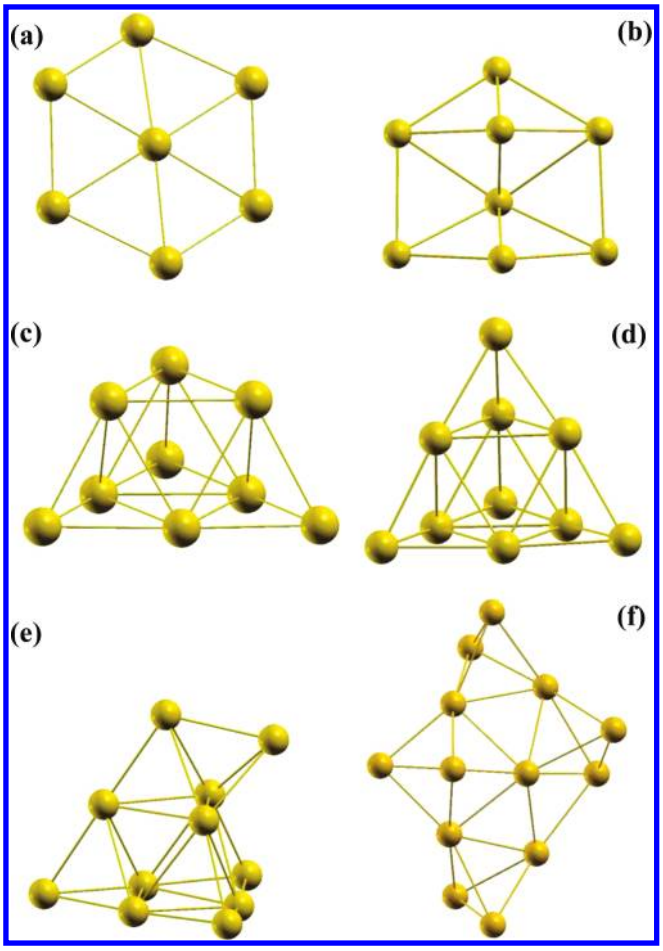

Figure 2. Lowest-energy isomers of bare gold clusters: (a) Au_7^{2+}, (b) Au_8^{2+}, (c) Au_9^{2+}, (d) Au_{10}^{2+}, (e) Au_{11}^{3+}, and (f) Au_{13}^{5+} clusters.

redistribution from the gold toward the ligands to be a key factor in ligand stabilization of the cluster geometry.[10] While we find similar effects for the bidentate-ligand-protected small gold clusters, we show that structural inflexibility of the bidentate ligands plays an additional critical role in determining the stability of gold nanoclusters. We describe our theoretical methods in section 2, present and discuss our results in section 3, and summarize our conclusions in section 4.

2. THEORETICAL METHODS

2.1. Model System. Our model systems consist of complexes of gold clusters Au_n^q ($n = 2-11; q > 0$) and diphosphine ligands $[P(Ph)_2(CH_2)_MP(Ph)_2]_x$ (M = 3, 5) which we designate as $Au_n(L^M)_x^q$, where n = number of gold atoms, x = number of ligands, M = spacer size, and q = charge state. For simplicity in calculations, we replace the phenyl group (C_6H_5) by H. To further test the validity of our conclusions we extend the calculations to Au_{13} cluster and employ a larger ligand (M = 10) for the interaction with the gold trimer. The structures of these three diphosphine ligands, $PH_2(CH_2)_3PH_2$ (henceforth termed L^3), $PH_2(CH_2)_5PH_2$ (henceforth termed L^5), and $PH_2(CH_2)_{10}PH_2$ (henceforth termed L^{10}), and that of phosphine are presented in Figure 1.

Our main interest in this work is in cationic Au_n ($n = 8-11$), which were synthesized selectively in recent experiments.[8,9] Understanding the stability of these gold nanoclusters requires insights from the electronic and geometric structures of both the bare metal clusters and their ligated counterparts for the smaller ($n = 2-7$) as well as for the larger ($n = 8-11$) sized ones produced in experiments. We have thus investigated ligand−gold complexes Au_n^q ($n = 2-11$; $q = 1-3$ depending on n), plus Au_{13}^q (q = 2, 3, 5), as a further test of our theory. We set the ionized state q to 2+ for Au_n^q ($n = 7-10$) clusters and to 3+ for the $n = 11$ cluster, to be in accord with those in experiments.[8,9] For n = 13 we set it to 5+, to satisfy the criterion for magic number. Thus, all of the studied gold clusters are cationic.

2.2. Geometry Optimization and Total Energy Calculations. We have performed scalar relativistic DFT calculations[11] using the plane wave basis set and the projector augmented wave pseudopotential method,[12] as implemented in the Vienna ab initio simulation package (VASP).[13] The wave functions are expanded in the plane wave basis with a kinetic energy cutoff of 400 eV. For the exchange−correlation energy, we use the Perdew−Burke−Ernzerhof functional.[14] We use a supercell of dimension 24 × 24 × 24 Å^3 for all gold clusters except $Au_{13}(L^5)_6^{q+}$ and $Au_{13}(L^{10})_6^{q+}$ (q = 2, 3, 5) complexes, for which we use a larger supercell of dimension 30 × 30 × 30 Å^3. Because of the large size of the supercells, only a single k-point is sufficient for the sampling of the Brillouin zone. We use a Fermi-level smearing of 0.2 eV for gold clusters. While we set the threshold for electronic energy convergence to 10^{-6} eV, we set that for structural optimization to 10^{-4} eV for energy and to 2×10^{-2} eV/Å for force convergence. We use a standard quasi-Newtonian algorithm implemented in VASP for structural optimization.

For the structural optimization of bare gold clusters Au_n^q (n = 2−11, 13), if the geometries of the cationic gold clusters are not known, we optimize those of the neutral or anionic counterparts (of course, with the aforementioned charge state q) and choose

dx.doi.org/10.1021/jp201723b |J. Phys. Chem. C 2011, 115, 14478–14487

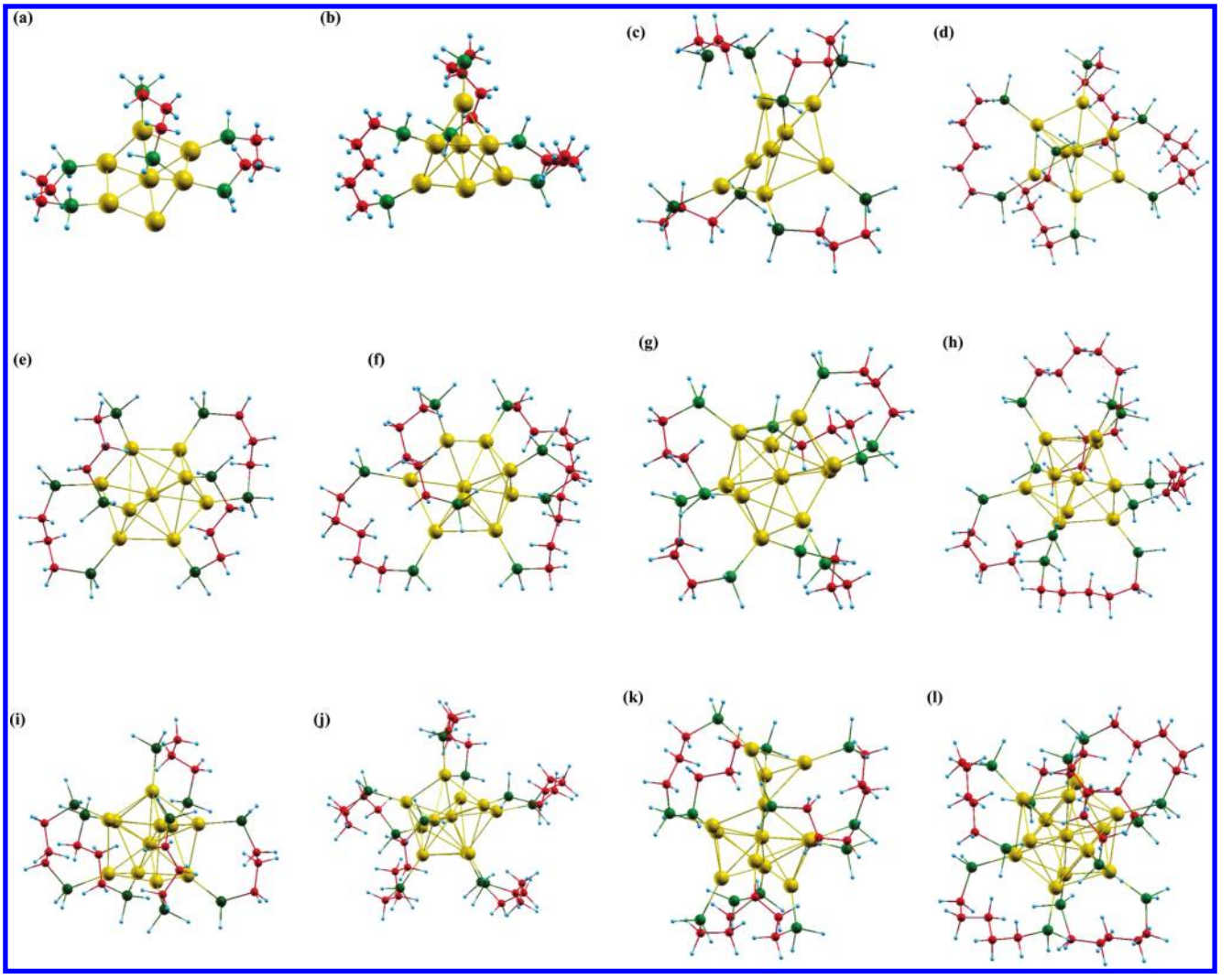

Figure 3. Lowest-energy isomers of diphosphine-protected gold clusters: (a) $Au_7(L^3)_3^{2+}$, (b) $Au_7(L^5)_3^{2+}$, (c) $Au_8(L^3)_4^{2+}$, (d) $Au_8(L^5)_4^{2+}$, (e) $Au_9(L^3)_4^{2+}$, (f) $Au_9(L^5)_4^{2+}$, (g) $Au_{10}(L^3)_5^{2+}$, (h) $Au_{10}(L^5)_5^{2+}$, (i) $Au_{11}(L^3)_5^{3+}$, (j) $Au_{11}(L^5)_5^{3+}$, (k) $Au_{13}(L^3)_6^{5+}$, and (l) $Au_{13}(L^5)_6^{5+}$ complexes.

the one that has the lowest energy. The neutral or anionic geometries that we used as initial geometries of cationic gold clusters include Au_n (n = 2, 3, 5, 7, 9, 13),[15] Au_n^q (n = 3, 4; q = 0, 1, −1),[16] and Au_n^{1-} (n = 4−11, 13).[17] Furthermore, for bare Au_8^{2+} and Au_{11}^{3+} clusters, we use a basin hopping algorithm[18] to find the lowest energy isomers. For structural optimization of the corresponding ligand-protected gold clusters, we optimize gold−ligand complexes that consist of the lowest-energy isomers of the bare gold clusters and the diphosphine ligands. For the ligated counterparts of Au_8^{2+}, Au_{10}^{2+}, and Au_{11}^{3+} complexes, we also optimize the experimentally available geometries[19−21] to confirm that the experimental geometries are favored (i.e., lower in energy) over the ones obtained from the optimization of simple ligation of the bare clusters. The optimized geometries for the bare clusters Au_n^q (n = 7−11, 13; q = 1−3 depending on n) are presented in Figure 2, and those for the gold−ligand complexes $Au_n(L^M)_x^q$ (M = 3, 5) are presented in Figure 3.

2.3. Correction to Total Energy of Charged Systems. Cluster suspensions generated by wet-chemical methods are usually charged. Therefore, we have paid special attention to the treatment of the nonneutral systems that consist of charged gold nanoclusters and neutral ligands. For such charged systems, the periodic supercell method cannot normally be employed. By introducing a compensating, homogeneous background charge with opposite sign, however, the charge can be balanced out. The resulting neutral supercell enables the application of periodic boundary conditions.[22−24] Interaction between the charged supercell and its periodic images causes spurious long-range Coulomb interaction, which slows down the convergence of total energy even for a supercell of fairly large dimension.[22] In order to tackle the issue of spurious interaction, and thereby that of slow convergence, a correction term is introduced on top of the total energy expression for the uncorrected system:

$$E^1 = E^0 + \frac{1}{2}\alpha Q^2/\varepsilon_0 D \qquad (1)$$

where E^0 and E^1 are the energies of the system of interest before and after the correction, respectively, and $^1/_2\alpha Q^2/\varepsilon_0 D$ is the correction term, in which α is the appropriate Madelung constant, Q is the total charge on the cluster, ε_0 is the dielectric constant, and D is the dimension of the cubic supercell.

Thus corrected, the total energy of a charged system is quite reliable, depending on the magnitude of q. We present the calculated ionization energy of gold monomer together with the

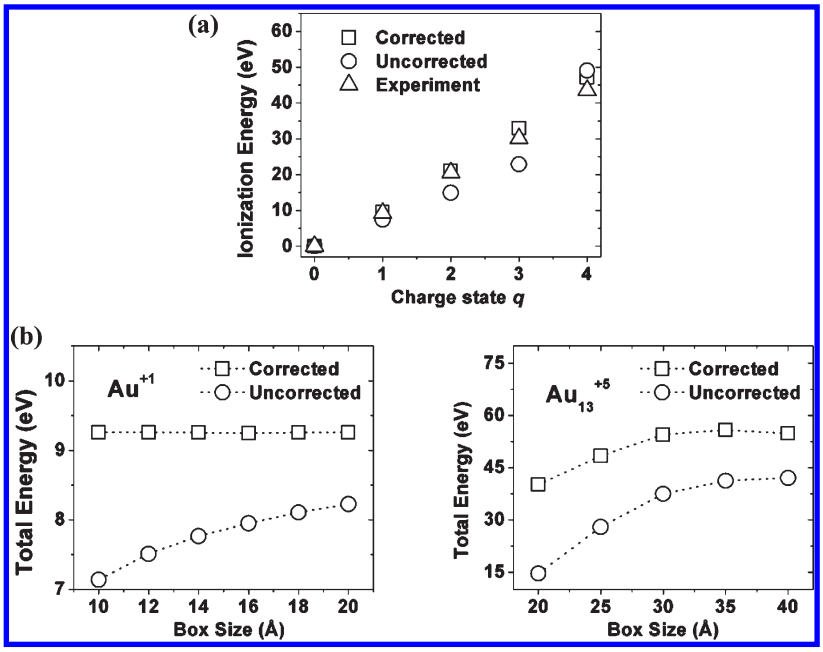

Figure 4. (a) Ionization energies for a single gold atom and (b) effect of charge correction scheme on the convergence of total energy as a function of supercell size for Au^{1+} monomer and $Au_{13}{}^{5+}$.

experimental data in Figure 4a. Before introduction of the charge correction described above, the calculated values are up to 30% off the experimental ones. After correction, the discrepancy is reduced to less than 10%. Figure 4b presents the total energies of Au^{1+} monomer and $Au_{13}{}^{5+}$ as a function of supercell size before and after the correction. For Au^{1+} monomer before the correction, the convergence of the total energy is slow as the dimension of the box increases, but after the correction it becomes very fast, enabling the usage of a fairly small supercell ($\leq$10 Å). For $Au_{13}{}^{5+}$ monomer, the correction is not so effective as that for Au^{1+}. Thus, while our supercell size (24 Å) is sufficient for small q, a larger supercell ($\geq$35 Å) is desirable for large q. However, since all gold clusters in this study have a q smaller than +5, except Au_{13}, the current correction scheme and choice of supercell should be quite sufficient. Note also that we used a large supercell of dimension 30 × 30 × 30 Å^3 for the particular cases of $Au_{13}(L^5)_6{}^{5+}$ and $Au_{13}(L^{10})_6{}^{5+}$ complexes. In fact, relative difference in total energies is the actual quantity of interest. Given the measures that we have taken, we believe the numerical errors associated with our calculations are not substantial for gold clusters with large q = +5.

2.4. Stabilization Condition. Confining ourselves to considerations of system energetics, we define *relative stability* (RS) as the difference in total energy between parent and child clusters in order to determine the stabilization of a particular size of gold cluster by diphosphine ligands of specific dimension:

$$\mathrm{RS} = E[\mathrm{Au}_n(\mathrm{L}^M)_x{}^q] - E[\mathrm{Au}_{n1}(\mathrm{L}^M)_{x1}{}^{q1}] - E[\mathrm{Au}_{n2}(\mathrm{L}^M)_{x2}{}^{q2}] \quad (2)$$

where $E[\mathrm{Au}_n(\mathrm{L}^M)_x{}^q]$, $E[\mathrm{Au}_{n1}(\mathrm{L}^M)_{x1}{}^{q1}]$, and $E[\mathrm{Au}_{n2}(\mathrm{L}^M)_{x2}{}^{q2}]$ are the DFT total energies of the parent and child clusters, respectively. RS < 0 for every $(n1, n2) \in n$ indicates that parent is stable, and the larger the magnitude of RS, the more stable the cluster. Thus, small negative RS means that parent cluster is prone to disintegration even under weak perturbation (for example, thermal vibrational energy). The conservation of the number of gold atoms ($n = n1 + n2$), and of the number of ligands ($x = x1 + x2$), and of the charges $q = q1 + q2$ are implicit in the stability condition (RS < 0).

As alluded to already, RS does not include any contribution of the activation energy required for the break-up of a parent cluster into child clusters. Rather, it includes only the total energies of initial and final states. In other words, we are not considering kinetic effects. As for vibrational entropy contribution, its net contribution to RS is only a few millielectronvolts[25] and therefore is negligible with respect to the magnitude of RS of the gold clusters studied here (>0.1 eV).

To evaluate RS, we need to know the number of ligands that coordinate to parent and child clusters, and also the charge states of parent and child clusters. The number of ligands, x, that coordinate to a cluster, whether parent or child, can be determined as follows:

$$x = \begin{cases} \dfrac{n}{2} & n = \text{even} \\ \dfrac{n-1}{2} & n = \text{odd} \end{cases} \quad (3)$$

where n is the number of gold atoms of the cluster. The above assignments, which are in accord with experiment,[8,9] guarantee that a diphosphine binds with two gold atoms. As a result, every gold atom in the even-size gold clusters is coordinated to by diphosphines, but one gold atom in the odd numbered gold clusters has no coordination. Cases exceptional to the assignment in eq 3 may include gold monomer, dimer, and trimer. In these very small gold clusters, the coordination number of ligands is often larger than half the number of Au atoms. We return to these interesting cases in section 3.5.

The thus-generated x, $x1$, and $x2$ should satisfy the conservation of ligand numbers in parent and child systems (i.e., $x = x1 + x2$). In some rare cases, when we assign the number of ligands according to eq 3, the resulting x, $x1$, and $x2$ do not satisfy the

Table 1. For Ligand−Gold Cluster Complexes $Au_n(L^M)_x^q$, x and q Values Associated with Each n

n	x	q
2	1	1, 2
3	1	1
4	2	1
5	2, 3	1
6	3	1, 2
7	3	1, 2
8	4	1, 2
9	4	2
10	5	2
11	5	3
13	6	2, 3, 5

Table 2. Calculated Total Energy and Relative Stability (RS) of Parent (Au_nL^3) and Child Clusters ($Au_{n1}L^3$ and $Au_{n2}L^3$)

parent (n)		child ($n1$, $n2$)				
n	E_n (eV)	$E_{n-2,2}$ (eV)	$E_{n-3,3}$ (eV)	$E_{n-4,4}$ (eV)	$E_{n-5,5}$ (eV)	RS (eV)
7	−228.79	−227.56	−228.92	a	a	0.13
8	−307.89	−303.61	−306.74	−307.31	a	−0.58
9	−310.63	−307.11	−308.13	−310.47	a	−0.16
10	−388.48	−384.93	a	−386.52	−388.29	−0.19
11	−383.33	−381.38	−383.17	−382.45	−382.50	−0.16
13	−438.67	−444.84	a	a	a	6.17

[a] Calculations were not performed for this particular combination of child clusters, as it violated a conservation rule.

conservation of ligands (i.e., $x > x1 + x2$). In such instances, we increase $x1$ (or $x2$ if necessary) in order to satisfy the conservation of ligands.

For the charge state of the clusters, since a gold cluster in solution tends to polarize, we assign $q \geq 1$ to all gold clusters ($q, q1, q2 \geq 1$). We thereby consider only cationic gold clusters in our calculations, as was the case in experiment.[8,9] As a result, the charge state of parent clusters is equal to or larger than +2 in order to satisfy charge conservation between parent and child clusters ($q = q1 + q2$). In Table 1 we summarize the n, x, and q values for the gold cluster complexes $[Au_n(L^M)_x^q]$ investigated in this study.

3. RESULTS AND DISCUSSION

We present first our calculated total energies of $Au_n(L^3)_x^q$ ($n = 7-11, 13$) in Table 2 and those of $Au_n(L^5)_x^q$ ($n = 7-11, 13$) in Table 3. Calculations were not performed for certain combinations of child clusters, as they violated a conservation rule. For example, (7,3) for Au_{10} is omitted since it violates the conservation of the number of ligands.

3.1. Interaction of L^3 with Au_n ($n = 7-11, 13$). From Table 2, we see that in the presence of ligand L^3 the most stable child clusters are (11,2) for Au_{13}^{5+}, (8,3) for Au_{11}^{3+}, (5,5) for Au_{10}^{2+}, (5,4) for Au_9^{2+}, (4,4) for Au_8^{2+}, and (4,3) for Au_7^{2+}. The last column in Table 2 gives the relative stability for each n. We find that stable parent clusters are Au_{11}^{3+}, Au_{10}^{2+}, Au_9^{2+}, and Au_8^{2+} with RS values of −0.16, −0.19, −0.16, and −0.58 eV, respectively. Our calculations thus predict stabilization of Au_{11}^{3+} by L^3, in agreement with experiment.[8,9] Our results, however, do not indicate exclusive selectivity of L^3 toward Au_{11}^{3+} as suggested in one experiment,[8] as the former seems to stabilize several other sizes as well. Regarding this discrepancy, it is noteworthy that another experiment, which used different solutions, reports that L^3 generates Au_8^{2+} in addition to Au_{11}^{3+}.[9] Selectivity of the ligands may thus depend to some extent on experimental conditions.

Table 3. Calculated Total Energy and Relative Stability of Parent (Au_nL^5) and Child Clusters ($Au_{n1}L^5$ and $Au_{n2}L^5$)

parent (n)		child ($n1$,$n2$)				
n	E_n (eV)	$E_{n-2,2}$ (eV)	$E_{n-3,3}$ (eV)	$E_{n-4,4}$ (eV)	$E_{n-5,5}$ (eV)	RS (eV)
7	−328.86	−328.04	−329.41			0.55
8	−441.02	−438.18	−439.6	−440.44	a	−0.58
9	−443.54	−441.22	−442.08	−442.98	a	−0.56
10	−553.71	−551.84	a	−553.12	−553.17	−0.54
11	−549.67	−548.83	−550.23	−549.09	−548.6	0.56
13	−639.74	−644.5	a	a	a	4.76

[a] Calculations were not performed for this particular combination of child clusters, as it violated a conservation rule.

Table 4. Decomposition of Total Energies of $Au_n(L^3)_x^q$ Complexes

n	$E(Au_{n1}^{q1})$ (eV)	$E(Au_{n2}^{q2})$ (eV)	$E(Au_n^q)$ (eV)	x_1BE_1 (eV)	x_2BE_2 (eV)	xBE (eV)	ΔE_{bare} (eV)	ΔBE (eV)
7	0.65	2.7	4.09	−7.57	−4.6	−12.78	0.74	−0.61
8	0.65	0.65	−1.79	−7.57	−7.57	−12.63	−3.09	2.51
9	−2.44	0.65	−2.48	−7.64	−7.57	−14.68	−0.69	0.53
10	−2.44	−2.44	−6.43	−8.93	−7.64	−15.21	−1.55	1.36
11	−1.79	2.69	5.41	−12.63	−4.6	−21.9	4.51	−4.67
13	5.41	19.85	37.33	−21.9	−8	−35.8	12.07	−5.9

3.2. Interaction of L^5 with Au_n ($n = 7-11, 13$). For $Au_n(L^5)_x$ complexes, we find in Table 3 that the most-stable child clusters are (11,2) for Au_{13}^{5+}, (8,3) for Au_{11}^{3+}, (5,5) for Au_{10}^{2+}, (5,4) for Au_9^{2+}, (4,4) for Au_8^{2+}, and (4,3) for Au_7^{2+}. Stable (parent) clusters turn out to be Au_{10}^{2+}, Au_9^{2+}, and Au_8^{2+} with RS of −0.54, −0.56, and −0.58 eV, respectively, in excellent agreement with experiment.[8,9] We find that Au_8^{2+} is the most stable among the stabilized gold clusters with the largest RS of −0.58 eV.

3.3. Contributions to Stability Condition. In sections 3.1 and 3.2, we reported that L^3 stabilizes Au_{11}^{3+}, Au_{10}^{2+}, Au_9^{2+}, and Au_8^{2+} clusters while L^5 stabilizes Au_{10}^{2+}, Au_9^{2+}, and Au_8^{2+} clusters. These conclusions were based on simple comparison of the total energies of the parent, $E[Au_n(L^M)_x^q]$, with those of child complexes, $E[Au_{n1}(L^M)_{x1}^{q1} + Au_{n2}(L^M)_{x2}^{q2}]$. Such consideration does not allow isolation of the factors that may be responsible for the stabilization. To get further insight, we evaluate the binding energies of all systems of interest here: gold−ligand complexes, bare gold clusters, and pure ligands. To begin with the total energy of the parent complex can be expressed as in the following:

$$E[Au_n(L^M)_x^q] = E(Au_n^q) + E(L_x^M) + x\text{BE} \quad (4)$$

where $E(Au_n^q)$ and $E(L^M_x)$ are the total energies of the bare gold

Table 5. Decomposition of Total Energy of $Au_n(L^5)_x^q$ Complexes

n	$E(Au_{n1}^{q1})$ (eV)	$E(Au_{n2}^{q2})$ (eV)	$E(Au_n^q)$ (eV)	x_1BE_1 (eV)	x_2BE_2 (eV)	xBE (eV)	ΔE_{bare} (eV)	ΔBE (eV)
7	0.65	2.7	4.09	−7.91	−5.4	−13.50	0.74	−0.19
8	0.65	0.65	−1.79	−7.91	−7.91	−13.31	−3.09	2.51
9	−2.44	0.65	−2.48	−7.91	−7.35	−15.13	−0.69	0.13
10	−2.44	−2.44	−6.43	−8.52	−7.35	−14.86	−1.55	1.01
11	−1.79	2.69	5.41	−13.31	−5.4	−22.66	4.51	−3.95
13	5.41	19.85	37.33	−22.66	−8.2	−38.17	12.07	−7.31

cluster and the ligands, respectively, and BE is the binding energy per ligand of the cluster. (Note that BE < 0 is required for bonding between gold clusters and ligands.) Similarly, the total energy of child complexes can be expressed as follows:

$$E[Au_{n1}(L^M)_{x1}{}^{q1} + Au_{n2}(L^M)_{x2}{}^{q2}] = E(Au_{n1}{}^{q1}) + E(Au_{n2}{}^{q2}) + E(L_{x1}^M) + E(L_{x2}^M) + x_1BE_1 + x_2BE_2 \quad (5)$$

where BE_1 and BE_2 are the binding energies per ligand for the child clusters. When we substitute eqs 4 and 5 into eq 2, the relative stability term automatically breaks up into a part arising from the ligands and another from the bare clusters:

$$RS = [xBE - (x_1BE_1 + x_2BE_2)] + \{E(Au_n{}^q) - [E(Au_{n1}{}^{q1}) + E(Au_{n2}{}^{q2})]\} \quad (6)$$

where the first term on the right represents the difference in the ligand−cluster interaction between parent and child complexes (ΔBE), while the second term is the total energy difference between *bare* parent and *bare* child clusters (ΔE_{bare}), which is unaffected by ligand−gold interaction. Thus,

$$RS = \Delta BE + \Delta E_{bare}. \quad (7)$$

Tables 4 and 5 show the decomposition of the total energies listed in Tables 2 and 3 into ΔBE and ΔE_{bare}, respectively. Importantly, ΔBE in Table 4 is positive for stable $Au_8(L^3)_4{}^{2+}$, $Au_9(L^3)_4{}^{2+}$, and $Au_{10}(L^3)_5{}^{2+}$ complexes and negative *only* for the $Au_{11}(L^3)_5{}^{3+}$ complex. Thus ligand−gold interactions (ΔBE) *do not* contribute to the stabilization of $Au_8(L^3)_4{}^{2+}$, $Au_9(L^3)_4{}^{2+}$, and $Au_{10}(L^3)_5{}^{2+}$. Rather, their stabilization arises simply from the superior stability of these bare parent clusters (with respect to that of the bare child clusters), since ΔE_{bare} in Table 4 is negative for these complexes. In other word, even without diphosphines, these clusters ($Au_8{}^{2+}$, $Au_9{}^{2+}$, and $Au_{10}{}^{2+}$) will be stable. As such, adding ligands does not change the picture. On the other hand, ligand−gold interaction is responsible for the stabilization of $Au_{11}L^3$. Interestingly, for $Au_{13}(L^3)_6{}^{5+}$, although ΔBE is negative and large, ΔE_{bare} is even larger. The overall result is that the complex is unstable.

Let us take a closer look at the unique $Au_{11}(L^3)_5{}^{3+}$ complex. Its large ΔE_{bare} indicates that the bare $Au_{11}{}^{3+}$ cluster is inherently unstable. However, ΔBE of this complex is negative, and larger than ΔE_{bare}. As a result, this complex is stable and the gold−ligand interaction is critical for the stabilization of this complex. Thus, we can conclude that, in terms of ligand-induced stabilization, $Au_{11}{}^{3+}$ is the only gold cluster to be stabilized by L^3 and that the strong interaction of L^3 with $Au_{11}{}^{3+}$ is the decisive factor in this selectivity.

When we bring the same analysis to bear on the $Au_n(L^5)_x{}^{q+}$ (x = 7−11, 13) complexes (cf. Table 5), we find that the stabilization of $Au_8(L^5)_4{}^{2+}$, $Au_9(L^5)_4{}^{2+}$, and $Au_{10}(L^5)_5{}^{2+}$ complexes also turns out to be of *nonligand* origin, as with $Au_8(L^3)_4{}^{2+}$, $Au_9(L^3)_4{}^{2+}$, and $Au_{10}(L^3)_5{}^{2+}$, since ΔBE for each of these complexes is positive. In summary, our analysis of ligand stabilization of gold clusters based on the stability condition (eq 7) reveals the true nature of the unique, ligand-induced stabilization of Au_{11} cluster by L^3, thereby confirming the selectivity of L^3 toward $Au_{11}{}^{3+}$ observed in experiment.[8]

3.4. Trends in Interaction of L^3 and L^5 with Cationic Gold Clusters. Figure 5a shows BE, the binding energy (per ligand) of $Au_n{}^q$ (n = 2−11, 13) complexes with L^M. Clearly, the interaction of diphosphines with gold clusters is size-dependent. Although that relationship is not simple, there are some trends: (1) L^5 generally has stronger interaction with gold clusters than L^3, except for $Au_{10}{}^{2+}$, $Au_8{}^{1+}$, and $Au_5{}^{1+}$. (2) L^3 and L^5 most strongly interact with $Au_2{}^{2+}$, $Au_2{}^{1+}$, $Au_{13}{}^{5+}$, and $Au_3{}^{1+}$. (3) Among gold clusters of interest, Au_n ($n \geq 7$), L^3 and L^5 interact most strongly with $Au_{13}{}^{5+}$, $Au_{11}{}^{3+}$, and $Au_7{}^{2+}$, which turn out to be the only gold clusters whose ΔBEs are negative (cf. Tables 4 and 5).

Figure 5b presents the energy gain (xBE) of each gold cluster from the interaction with ligands, which is obtained by multiplying the binding energy in Figure 5a by the number of ligands (Table 1). Clearly, $Au_{13}{}^{5+}$ and $Au_{11}{}^{3+}$ stand out with the largest energy gain from interaction with L^3 and L^5. Although $Au_2{}^{2+}$, $Au_2{}^{1+}$, and $Au_3{}^{1+}$ have large binding energy *per ligand*, since the number of ligands is small, the net energy gain is small.

It is interesting to note that nearly all of the most strongly interacting gold clusters—$Au_{13}{}^{5+}$, $Au_{11}{}^{3+}$, $Au_3{}^{1+}$, and $Au_2{}^{2+}$—possess a closed electronic shell configuration. Note that $Au_{13}{}^{5+}$ and $Au_{11}{}^{3+}$ acquire spherical geometries in $Au_{13}(L^M)_6{}^{5+}$ and $Au_{11}(L^M)_5{}^{3+}$ complexes (M = 3, 5). An exceptional case is $Au_{13}(L^3)_6{}^{5+}$, in which $Au_{13}{}^{5+}$ splits, as we shall discuss later. It is well-known that ligand-protected gold clusters show a preference for spherical geometry (for example, icosahedral Au_{13}).[26−28] The rationale for the stabilization (by phosphine ligand) in the case of neutral icosahedral Au_{13} cluster is the effective mixing of the orbitals of the gold atoms with those of the phosphorus atoms for spherical geometries, which redistributes charge from the gold cores toward the ligands.[10] We find a similar charge redistribution for the diphosphine-protected gold clusters, as shown in the Supporting Information. In summary, substantial charge accumulation occurs along the Au−P bonds as a result of charge depletion from the Au atoms, and thereby the central gold atom is charged positively, and both the peripheral gold atoms and diphosphines together are charged negatively, effectively forming an electronic core−shell structure similar to that of atoms in which the nucleus constitutes the positive inner core and electrons form the negative outer shell. This core−shell structure enhances the stability of the gold cluster, both because it enables the formation of electrostatic ionic bonding and because the outer shell can screen the inner core from interactions with external species, which could reconfigure the structure of the gold cluster.[29]

Regarding the interaction of diphosphines with the gold clusters, L^5 shows, in general, a stronger interaction with gold clusters than L^3. It is quite striking to observe such a consistent superiority of L^5 in view of the fact that the only difference between them is the length of spacer; that is, that the spacer of L^5 has an additional two CH_2 molecules in comparison with L^3. We attribute this superiority of L^5 over L^3 to strain effect originating

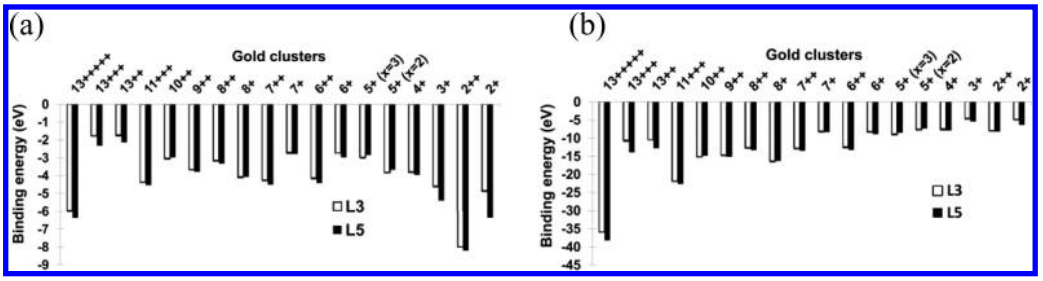

Figure 5. (a) Binding energy *per ligand* and (b) energy in the formation of $Au_n(L^M)_x^q$ complexes. The charge states of the gold cores, q, are represented as plusses in the graph. For the number of diphosphines, x, refer to Table 1.

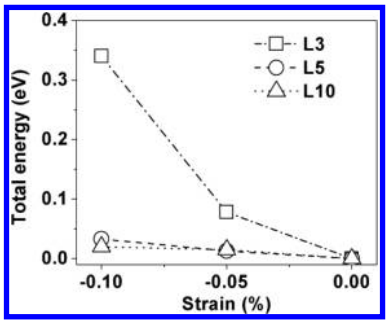

Figure 6. Change in total energies of L^3, L^5, and L^{10} with applied strain.

from the stiffness of spacer, as we discuss in the section that follows.

3.5. Ligand Flexibility and Structural Stabilization. When a diphosphine attaches to a gold cluster, it experiences a bending of the spacer (i.e., strain). Since such bending involves bond-length change, it will increase the total energy of the ligand. Such total energy increase will, however, be small if a diphosphine is flexible. Flexibility of a diphosphine can stem from a large degree of freedom in its structure, which is brought about by many numbers of CH_2 chains in the spacer. To demonstrate the correlation of flexibility with the length of spacer, we performed a series of calculations in which we applied a set of strains to a pool of diphosphines with different spacers, namely, L^3, L^5, and L^{10}. Length, which is defined as the sum of P−C and C−C bond lengths, is 6.84, 9.88, and 17.54 Å for L^3, L^5, and L^{10}, respectively. We calculate ligand stress (σ), as a measure of flexibility, using the following equation:

$$\sigma = \frac{1}{L}\frac{dE}{d\varepsilon} \tag{8}$$

where L and E are the length and total energy of diphosphines, respectively, and ε is strain. We apply strain of −5% and −10%. Figure 6 shows the total energy change with respect to the applied strain for L^3, L^5, and L^{10}. It is clear that the smaller the length of spacer, the larger the total energy increase and so the induced stress. The calculated stress for L^3, L^5, and L^{10} is 0.227, 0.026, and 0.017 eV/Å, respectively. A stress imposed on L^3 is larger by an order of magnitude than that on either L^5 or L^{10}. As such, L^3 is by far stiffer than either L^5 or L^{10}. Thus, the impact of the length of spacer on the stress (and thereby on the flexibility) is remarkable. The longer the length of spacer, the more flexible the ligand. Note, however, that the stress quickly converges as the spacer length increases.

To further investigate the flexibility of ligand with variation of the length of spacer, we performed another set of calculations in which L^3, L^5, and L^{10} and phosphine ligands interact with a reference gold cluster, gold trimer (Au_3). Figure 7a displays such a configuration. We chose gold trimer as reference system since the diphosphine-gold bonding involves a single central gold atom to which peripherals are bonded. We fix the Au−Au bond length (d_{Au-Au} in Figure 7a) at the prescribed values (2.0, 2.5, 3.0, and 3.5 Å), and then completely relax the gold−ligand complex. We present the resulting Au−P bond length (d_{Au-P}) and the Au−Au−P bond angle (θ) in Figure 7b and 7c, respectively. In terms of d_{Au-P} and θ, the structural characteristics of L^{10} are the most similar to those of the phosphine. In contrast, the structural characteristics of L^3 are markedly different from those of the phosphine and others. Thus, we find a trend that the longer the ligand, the more similar the structural characteristics to those of the phosphine. The reason is clear: since phosphine itself can be considered to be infinitely flexible owing to its lack of spacer, the more flexible a diphosphine, the more closely it resembles phosphine.

Then the question thus arises as to whether the ligands with different spacer lengths show drastically different responses to external strain because the spacer fundamentally alters the electronic structure of diphosphines. Figure 8 shows the local density of states (LDOS) for the p orbital of the P atom of the phosphine and diphosphines (L^3, L^5, and L^{10}). The energy "0" eV in Figure 8 represents the energy of highest occupied molecular orbitals (HOMOs) of the relevant ligands. There are three sharp peaks (labeled I, II, and III from the right) in the case of phosphine. Similarly, we notice one sharp peak (labeled II) and two bands of peaks (labeled I and III from the right) in the case of diphosphines.

The three features of diphosphines in the LDOS can be unambiguously associated with the corresponding three peaks of phosphine. While peak II of diphosphines is nearly identical to that of the phosphine, peaks I and III are broadened from the corresponding peaks of the phosphine. The broadening of peaks I and III of diphosphines stems from the hybridization of the orbitals of P atom with those of spacers. Peak II, which is not broadened and is found at the location identical to that of the corresponding peak of phosphine, represents unpaired electrons of the P atom. The energy levels of these electrons are the HOMO energy levels of the ligand and thus are those primarily responsible for interaction with the gold cluster. The similarities of the electronic structures of L^3 and L^5 explain why L^3 and L^5 exhibit similar characteristics in the interaction with gold clusters, as discussed above (cf. Figure 5a). Since peak III represents the energy levels from the P−C and C−C interactions, these are

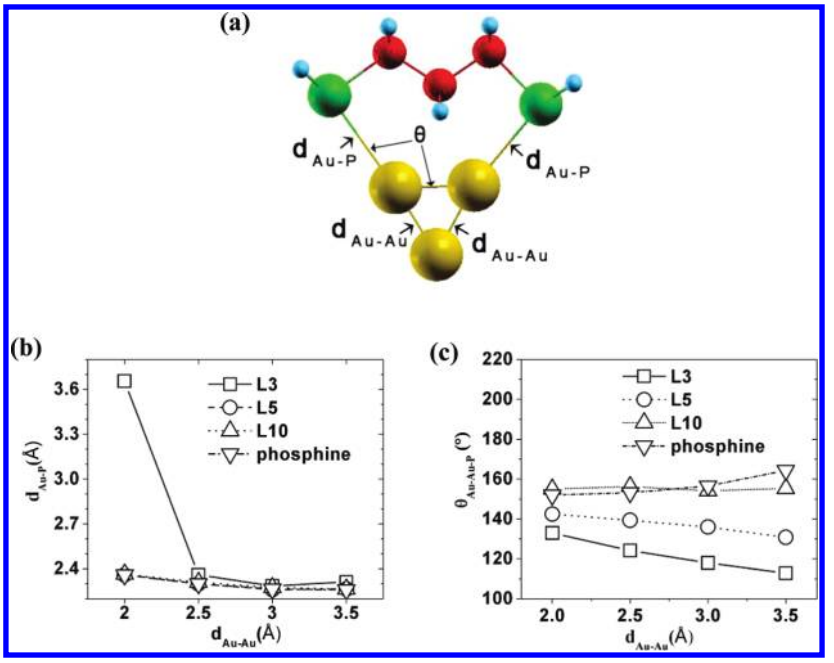

Figure 7. (a) Schematic model of the interaction of a reference gold trimer with diphosphines (only L^3 is shown). Calculated (b) Au−P bond length (d_{Au-P}) and (c) Au−Au−P bond angle (θ) are shown for simple phosphine and disphosphines (L^3, L^5, and L^{10}).

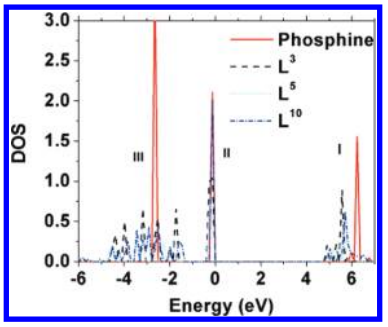

Figure 8. Local density of states of L^3, L^5, L^{10}, and phosphine.

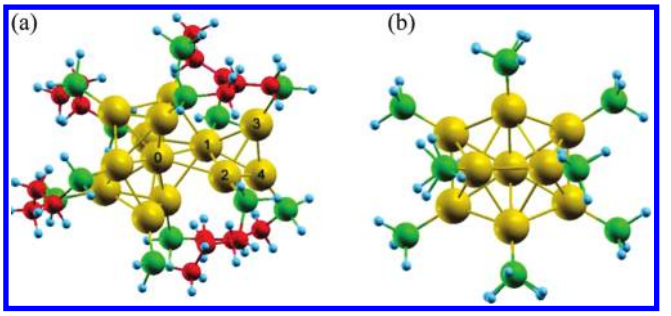

Figure 9. Optimized geometries of (a) $Au_{13}(L^3)_6^{5+}$ and (b) $Au_{13}(PH_3)_6^{5+}$.

related to the spacer-induced strain effect. The application of physical strain to spacers perturbs these energy levels, which lie relatively far beneath the HOMO energy (as compared to peak II). Therefore, they do not contribute directly to the interaction of the ligands with gold clusters as significantly as in peak II. That their contribution to the total energy of the system comes mainly through modified P−C and C−C interaction owing to applied strain explains the consistent superiority of flexible L^5 over stiff L^3.

A remarkable manifestation of the stiffness of L^3 is displayed in the core fission of the $Au_{13}(L^3)_6^{+5}$ complex. Figure 9 presents the optimized geometry of $Au_{13}(L^3)_6^{+5}$, which is split into two gold cores (Au_{10} and Au_3). Au 2, Au 3, and Au 4 form the split Au_3 core and the rest of the remaining gold atoms form the Au_{10} core. (Note that Au 1 is a bridging atom connecting the separated cores, and Au 0 is initially the central atom.) Imporantly, this remarkable gold-core fission occurs neither with L^5 nor L^{10} nor phosphine. In fact, these ligands stabilize the icosahedral geometry of Au_{13}^{5+} cluster. Thus, there is a clear distinction between L^3 and the rest of the ligands considered here, and the inference is that the stabilization ability of diphosphine is correlated to the flexibility of the ligand, so that the more flexible the ligand, the more stabilization capacity. On the basis of this correlation, we conclude that, in terms of stabilization (but not selectivity) ability, phosphine is superior to diphosphine, and L^{10} and L^5 are superior to L^3. Indeed, phosphine generates broad-range, polydisperse gold clusters.[8]

It is noteworthy that the remarkable effect of ligand-induced strain effect on stabilization of gold clusters is related to the peculiar bonding tendency of phosphine and gold. When we compare the geometries of $Au_{13}(L^3)_6^{5+}$ in Figure 9a and $Au_{13}(PH_3)_{12}^{5+}$ in Figure 9b, it is clear that phosphine ligands (PH_3) in Figure 9b tend to make a straight bond with the gold. (Note the straight lines connecting the central Au, any given surface Au, and the P atoms beyond it.) Now let us suppose that we add a spacer, like that of L^3 in the picture, between the pairs of two phosphines. (This operation basically transforms phosphines in Figure 9b to L^3 diphosphines in Figure 9a. The separations between the phosphine pairs in Figure 9b (the distance between the P atoms) are in the range of 5.35−5.62 Å (the average being 5.44 Å, which is smaller by 3.8% than the P−P separation of L^3 or L^5). Therefore, the connecting spacer (L^3 diphosphine) will be

under significant strain (−3.8%), which will in turn exert a strain (+3.8%) to the gold (cf. Figure 6 for stress). As a result, there will arise a competition between bending of the spacer (diphosphine) and expansion of the bond lengths of Au atoms that are bound to the diphosphine. In the case of $Au_{13}(L^3)_6^{5+}$, the strain induced by the stiff L^3 spacer causes the gold cluster to disintegrate.

Another example of the effect of the ligand-strain effect in gold−ligand complexes would be very small gold clusters Au_n (n = 2, 3). In experiment, Au_n ($1 \le n \le 3$) clusters are often observed with two or three diphosphines, indicating the binding of one or more diphosphines per gold atom. The bond lengths in the small gold clusters are relatively small (≈2.6 Å), enough to cause large strain upon the ligand. A possible way to relieve such strain is that only one end of the diphosphine binds to the gold cluster. This single-end binding will remove the source of strain. In such binding, diphosphine effectively acts as phosphine. Moreover, for further stabilization, the gold core can attract one or more additional diphosphines, since the uncoordinated gold atom is available for binding. As a matter of fact, such single-end binding is predicted in our calculations for the interaction of L^3 with the gold trimer: one end of the diphosphine is detached from the trimer. [Note the large average d_{Au-P} of 3.65 Å for L^3 (□ in Figure 7b) when d_{Au-Au} is 2.0 Å.]

3.6. Effect of Ligand Strain upon Selectivity of Diphosphine toward Specific Gold Clusters. We have shown that Au_{11}^{3+} is stabilized only by L^3 and not by L^5. However, in light of the fact that Au_{11}^{3+} interacts more effectively with L^5 than with L^3 as shown in Figure 5a, this result may seem odd. This contrasting behavior of L^3 and L^5 for Au_{11}^{3+} stems from the difference in ΔBE between $Au_{11}^{3+}(L^3)$ and $Au_{11}^{3+}(L^5)$: the magnitude of ΔBE for $Au_{11}^{3+}(L^3)$ (−4.67 eV) is larger than that for $Au_{11}^{3+}(L^5)$ (−3.95 eV). In fact, individual xBE, x_1BE$_1$, and x_2BE$_2$ values for $Au_{11}^{3+}(L^5)$ (in Table 5) are larger than those for $Au_{11}^{3+}(L^3)$ (in Table 4). This reversal can happen since ΔBE is the difference among those individual BEs, defined as $x\text{BE} - (x_1\text{BE}_1 + x_2\text{BE}_2)$. By comparing xBE, x_1BE$_1$, and x_2BE$_2$ for $Au_{11}^{3+}(L^5)$ in Table 5 with those for $Au_{11}^{3+}(L^3)$ in Table 4, we notice that the magnitudes of xBE, x_1BE$_1$, and x_2BE$_2$ for $Au_{11}^{3+}(L^5)$ are almost *uniformly* larger than those for $Au_{11}^{3+}(L^3)$ by 0.76, 0.8, and 0.68 eV, respectively. Owing to this uniformity, ΔBE of $Au_{11}^{3+}(L^3)$ becomes *larger* by 0.72 eV than that of $Au_{11}^{3+}(L^5)$. Clearly, the consistency of larger magnitude of xBE, x_1BE$_1$, and x_2BE$_2$ for L^5 than those of L^3 arises from *the spacer-induced strain effect* discussed in the previous section. Thus the ligand-induced strain plays a decisive role in selectivity of L^3 toward Au_{11}^{3+}.

3.7. Effect of Core Charges on Stability of Charged Gold Clusters. So far we have discussed the ligand-induced stabilization effect and have identified the critical, dominant role played by ligand-induced strain in selectivity. The relevant term is ΔBE in eq 7. However, we note that the selecting and stabilizing power of diphosphine—for example, that of L^3—is not only the result of this single factor (however dominant). Rather, it is the effect of a delicate balance among three factors: gold−ligand interaction, spacer-induced strain, and gold-core instability. In general, gold clusters with higher cationic state interact better with diphosphines than those with lower cationic state (cf. Figure 5a). For example, the binding energy of L^3 and L^5 for $Au_{13}(L^M)_6^{5+}$ is larger than that for $Au_{13}(L^M)_6^{2+}$ and $Au_{13}(L^M)_6^{3+}$. The only exception is $Au_8(L^M)_4^{q+}$ complexes.

Also, gold−ligand complexes of large q show higher values of ΔBE than those of small q, suggesting better stability for gold−ligand complexes of large q. For example, ΔBE in $Au_{13}(L^3)_6^{q+}$ complexes is −5.9 eV for q = +5, while they are 13.57 and 9.54 eV for q = +2 and +3, respectively. However, gold clusters with large q have large ΔE_{bare} as well, since such a large cationic core is by itself unstable. As a result, the RSs of $Au_{13}(L^3)_6^{q+}$ complexes (q = 2, 3, 5) are 8.02, 4.04, and 6.18 eV, while those of $Au_{13}(L^5)_6^{q+}$ complexes (q = 2, 3, 5) are −1.09, 1.24, and 4.77 eV. Thus, none of the $Au_{13}(L^M)_6^{q+}$ (q = 3 and 5; M = 3 and 5) complexes with high q is stable. It is clear that ligand−gold interaction (ΔBE) must be strong enough to override the large repulsive energy (ΔE_{bare}) for ligand-induced stabilization of gold cores of high q.

4. CONCLUSIONS

We have discussed stabilizing factors of ligand and nonligand origins. By nature the attractive ligand−gold interaction promotes gold core stability while the repulsive interaction within the core reduces the stability. Thus, there is the competition between two forces of contradicting nature in stabilization of the gold−ligand complexes. On the other hand, selectivity of ligands is different from the stabilization effect of ligands. A ligand can stabilize gold clusters of various sizes; however, this broadness demonstrates little selectivity. In this regard, selectivity is more complex a concept than stabilization. Nevertheless, the strong ligand−gold interaction, which defines stabilizing ability of ligands, is essential for selectivity.

Apparently, in order that a ligand can possess size-selecting power, the ability for the formation of strong gold−ligand interactions should be restricted to a narrow range of gold clusters. Here phosphine and diphosphine are two excellent prototype systems that exhibit broad and narrow interaction abilities, respectively. Simple phosphine strongly interacts with gold clusters due to its ability to make covalent bonding with gold clusters and is thus the representative of the high reactivity of an ideal selective ligand system.

On the other hand, it is the stiffness of spacer that is of critical importance concerning selectivity through induction of elastic strain. (In this aspect, L^3 is more selective than L^5.) Phosphine without the restricting power of spacer will be of no value regarding selectivity. Therefore, diphosphine having the power of reactive phosphine and, at the same time, the power of restrictive spacer as well is an effective size-selective system for gold clusters.

For an ideal, highly selective ligand, therefore, we propose a two-body ligand system, in which one part of the ideal ligand provides high reactivity toward the broad range of gold clusters and the other part of the ideal ligand provides control over the reactivity. This control could be in the form of a short length of spacer, as in diphosphine, or any type of controllable, reactivity-poisoning component. The controllable competition between the two components of an ideal, highly selective ligand system will produce a desirable selectivity for the generation of monodisperse nanoclusters of interest through a tailoring process.

■ ASSOCIATED CONTENT

Supporting Information. One figure showing charge-density difference isosurfaces of $Au_7(L^3)_3^{2+}$, $Au_7(L^5)_3^{2+}$, $Au_8(L^3)_4^{2+}$, $Au_8(L^5)_4^{2+}$, $Au_9(L^3)_4^{2+}$, $Au_9(L^5)_4^{2+}$, $Au_{10}(L^3)_5^{2+}$, $Au_{10}(L^5)_5^{2+}$, $Au_{11}(L^3)_5^{3+}$, $Au_{11}(L^5)_5^{3+}$, $Au_{13}(L^3)_6^{5+}$, and $Au_{13}(L^5)_6^{5+}$ complexes. This material is available free of charge via the Internet at http://pubs.acs.org.

■ ACKNOWLEDGMENT

We gratefully acknowledge financial support from the Department of Energy, Basic Energy Sciences (DE-FG02-07ER46354). We are indebted to Lyman Baker for many helpful remarks and critical reading of the manuscript.

■ REFERENCES

(1) Bond, G. C.; Thompson, D. T. *Catal. Rev. Sci. Eng.* **1999**, *41*, 319.
(2) Hughes, M. D.; Xu, Y.; Jenkins, P.; McMorn, P.; Landon, P.; Enache, D. I.; Carley, A. F.; Attard, G. A.; Hutchings, G. J.; King, F.; Stitt, E. H.; Johnston, P.; Griffin, K.; Kiely, C. J. *Nature* **2005**, *437*, 1132.
(3) Schaaff, T. G.; Whetten, R. L. *J. Phys. Chem. B* **2000**, *104*, 2630.
(4) Briant, C. E.; Hall, K. P.; Wheeler, A. C.; Mingos, D. M. P. *J. Chem. Soc., Chem. Commun.* **1984**, 248.
(5) Smits, J. M. M.; Bour, J. J.; Vollenbroek, F. A. *J. Cryst. Spectrosc.* **1983**, *13*, 355.
(6) Negishi, Y.; Takasugi, Y.; Sato, S.; Yao, H.; Kimura, K.; Tsukuda, T. *J. Am. Chem. Soc.* **2004**, *126*, 6518.
(7) Yanagimoto, Y.; Negishi, Y.; Fujihara, H.; Tsukuda, T. *J. Phys. Chem. B* **2006**, *110*, 11611.
(8) Bertino, M.; Sun, Z.; Zhang, R.; Wang, L. *J. Phys. Chem. B* **2006**, *110*, 21416.
(9) Bergeron, D. E.; Hudgens, J. W. *J. Phys. Chem. C* **2007**, *111*, 8195.
(10) Shafai, G.; Hong, S.; Bertino, M.; Rahman, T. S. *J. Phys. Chem. C* **2009**, *113*, 12072.
(11) Payne, M. C.; Teter, M. P.; Allan, D. C.; Arias, T. A.; Joannopoulos, J. D. *Rev. Mod. Phys.* **1992**, *64*, 1045.
(12) Blöchl, P. E.; Först, C. J.; Schimpl, J. *Bull. Mater. Sci.* **2003**, *26*, 33.
(13) Kresse, G.; Furthmüller, J. *Phys. Rev. B* **1999**, *54*, 11169.
(14) Perdew, J. P.; Burke, K.; Ernzerhof, M. *Phys. Rev. Lett.* **1996**, *77*, 3865.
(15) Shafai, G. S.; Shetty, S.; Krishnamurty, S.; Shah, V.; Kanhere, D. G. *J. Chem. Phys.* **2007**, *126*, No. 014704.
(16) Kryachko, E. S.; Remacle, F. J. *Chem. Phys.* **2007**, *127*, No. 194305.
(17) Hakkinen, H.; Yoon, B.; Landman, U.; Li, X.; Zhai, H.; Wang, L. *J. Phys. Chem. A* **2003**, *107*, 6168.
(18) Chuang, F. C.; Wang, C. Z.; Ogut, S.; Chelikowsky, J. R.; Ho, K. M. *Phys. Rev. B* **2004**, *69*, No. 165408.
(19) van der Velden, J. W. A.; Bour, J. J.; Bosman, W. P.; Noordik, J. H. *Inorg. Chem.* **1983**, *22*, 1913.
(20) Briant, C. E.; Hall, K. P.; Wheeler, A. C.; Michael, D.; Mingos, P. *J. Chem. Soc., Chem. Commun.* **1984**, 248.
(21) Smits, J.; Bour, J. J.; Vollenbroek, F. A.; Beurskens, P. T. *J. Cryst. Spectrosc.* **1983**, 13.
(22) Leslie, M; Gillan, M. J. *J. Phys. C: Solid State Phys.* **1985**, *18*, 973.
(23) Fuchs, K.; Wills, H. H. *Proc. R. Soc. A* **1935**, *151*, 585.
(24) Makov, G.; Payne, M. C. *Phys. Rev. B* **1995**, *51*, 4014.
(25) Yildirim, H.; Kara, A.; Rahman, T. S. *J. Phys.: Condens. Matter* **2009**, *21*, 084220.
(26) Van Der Velden, J. W. A.; Bour, J. J.; Bosman, W. P.; Noordik, J. H. *Inorg. Chem.* **1983**, *22*, 1913.
(27) Van Der Velden, J. W. A.; Beurskens, P. T.; Bour, J. J.; Bosman, W. P.; Noordik, J. H.; Kolenbrander, M.; Buskes, J. A. K. M. *Inorg. Chem.* **1984**, *23*, 146.
(28) Smits, J. M. M.; Bour, J. J.; Vollenbroek, F. A.; Beurskens, P. T. *J. Cryst. Spectrosc.* **1983**, *13*, 355.
(29) Verwey, E. J. W.; Overbeek, J. T. G. *Theory of the Stability of Lyophobic Colloids*, 2nd ed.; Dover Publications: Mineola, NY, 1999.